

Electronic Supplementary Information

Ionic-liquid assisted architecture of amorphous nanoporous zinc-rich carbon-based microstars for lithium storage

Experimental section

Preparation of the hierarchical nanoporous carbon materials

First, 0.1 mol $\text{Zn}(\text{OAc})_2 \cdot 2\text{H}_2\text{O}$ was dissolved 17.7g N,N-dimethylethanolamine (DMEA) and stirred for 12h under room temperature to form Zn(II)-rich ionic liquid. Then, the ionic liquid was added into 250-300 mL deionized water to obtain a clean solution. When the above solution becomes cloudy at 60 °C. 2-methylimidazole (2-MI, 0.1 mol) was added into the above solution and continued to be stirred until it becomes a milky and cloudy homogeneous solution. The resultant solid precipitates were collected and dried at 60 °C for 12h. Afterward, the precipitates were annealed at 650, 700, and 750°C (named Zn-N-C-1-700, Zn-N-C-1-650, Zn-N-C-1-750 respectively) for 5h under N_2 atmosphere with a heating rate of 5 °C/min starts from room temperature. N-C-1-700 was obtained from Zn-N-C-1-700 after acid washing with 1M HCl. Moreover, more 2-MI (0.2 mol) and other conditions are remained to get the sample annealed at 700°C for 5h (named Zn-N-C-2-700) in N_2 atmosphere. Meanwhile, after precipitates annealed at 500°C for 5h in air, pure ZnO was obtained and used as a referenced material.

Materials characterization

All X-ray diffraction (XRD) data were examined by the X-ray diffraction analysis system (D/MAX 2500V, Rigaku) equipped with a Cu-K α Radiation source ($\lambda=1.54056 \text{ \AA}$). The particle size and morphology of the ZIF-8 composite were investigated by using scanning electron microscopy (SEM) and the transmission electron microscopy (TEM) were obtained with JEOL JEM-1400 and JEOL 2100F. N₂ adsorption-desorption isotherms were conducted at 77 K on a Micromeritics Tristar 3000 analyzer. The BET surface areas and pore-size distribution curves were concluded using adsorption data. X-ray photoelectron spectroscopic (XPS) measurements were carried out by using a monochromated Al K α (1486.7 eV) X-ray source at the power of 150 W (15 kV \times 10 mA).

Electrochemical measurements

Electrochemical measurements were carried out in half cells at room temperature. Electrochemical tests were using coin cells (CR2032) with 1 mol/L LiPF₆ in EC/DMC (1:1 by volume) as electrolyte and lithium foil as counter and reference electrodes. Active material, and graphene electric oily slurry with a weight ratio of 8:2. The slurry was painted on aluminum foils fabricating the cathode through dried at 80 °C for 10 h. All cells were assembled in the Ar-filling glove box. Cyclic voltammograms (CV, 0.01–3 V) curves were measured at a scanning speed of 0.5 mV s⁻¹ by electrochemical workstations (DH7000 and CHI760E). The EIS measurements were performed with a 5 mV s⁻¹ voltage amplitude over a frequency range of 0.02 Hz to 100 kHz. Galvanostatic charge/discharge cycling was conducted using a battery

tester (Neware) at different current rates of 0.2 A g⁻¹ to 4 A g⁻¹.



Fig. S1. FESEM image of Zn-N-C-1 microstars.

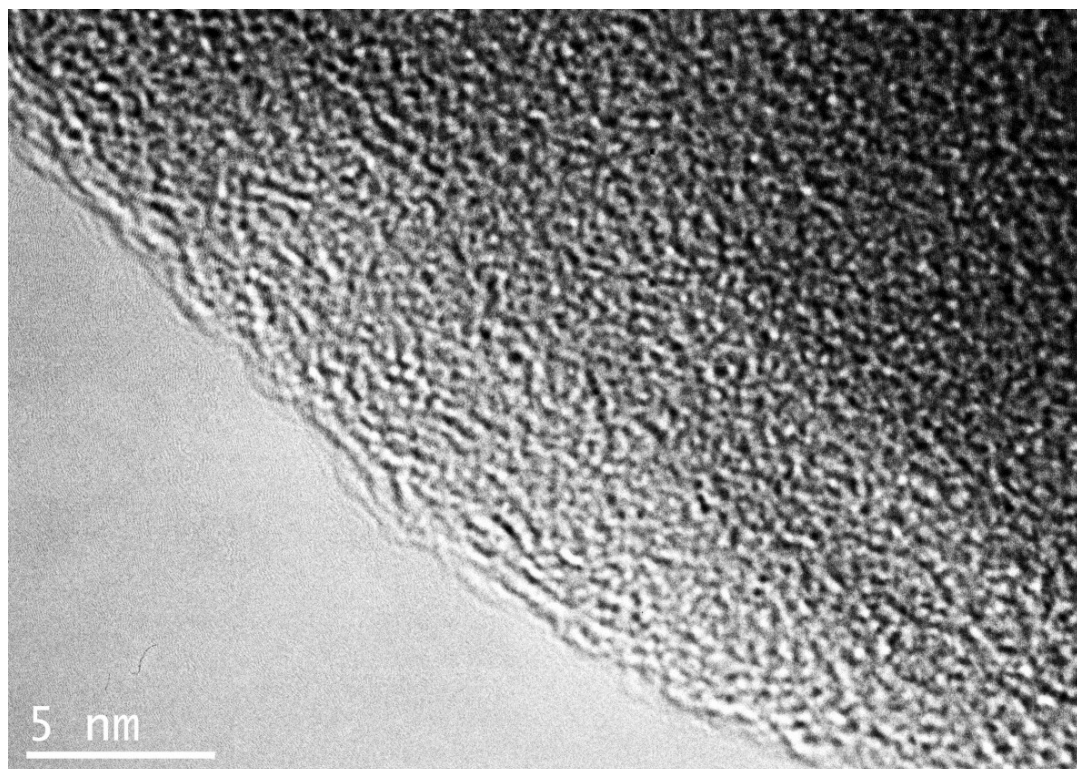


Fig. S3. HRTEM image of Zn-N-C-1-700.

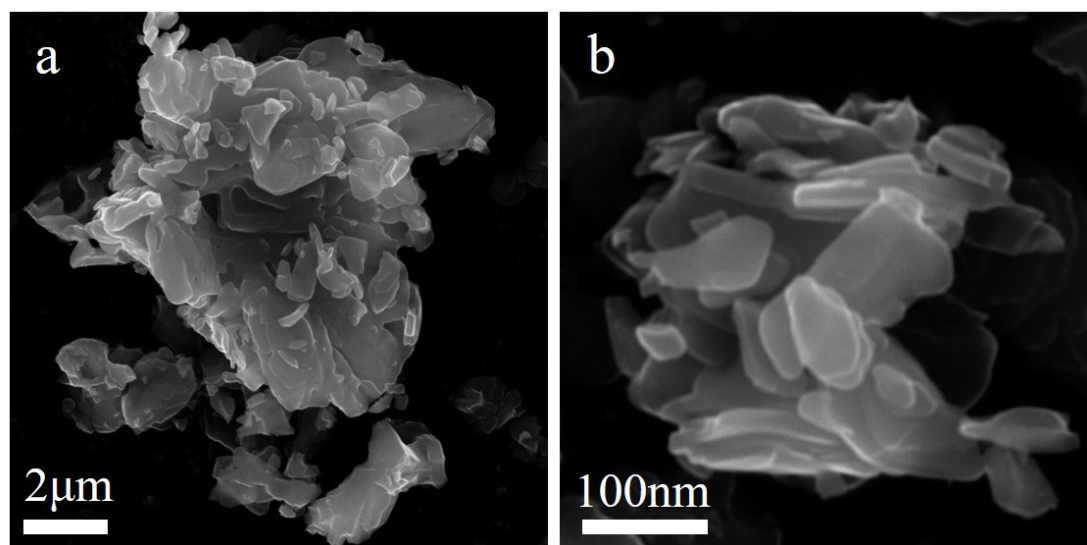


Figure. S3. (a, b) SEM images of the porous Zn-N-C-2-700 material in different magnifications.

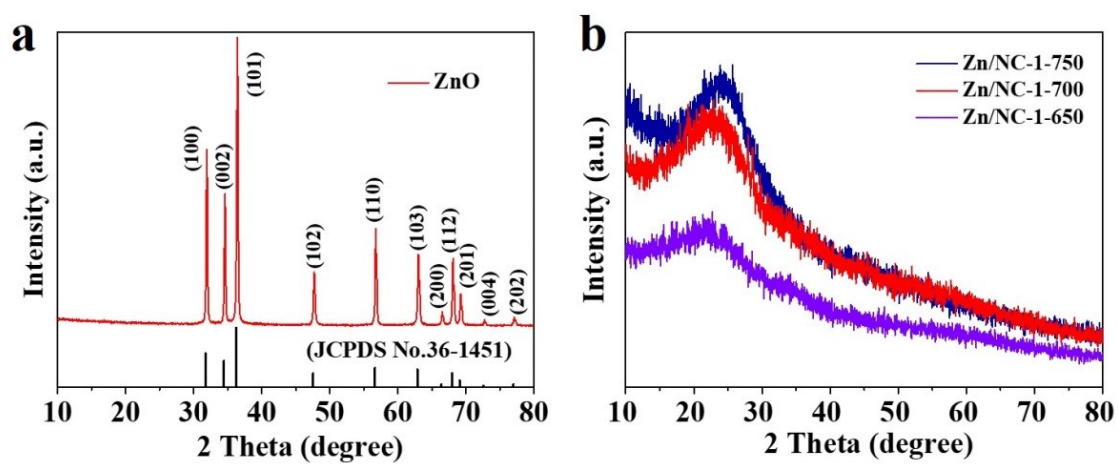


Fig. S4. (a) XRD pattern of ZnO; (b) XRD patterns of Zn-N-C-1-650, Zn-N-C-1-700, and Zn-N-C-1-750.

Table S1. Elemental composition determined by XPS.

| Sample | C1s (atom%) | N1s (atom%) | O1s (atom%) | Zn2p (atom%) |
|--------------|-------------|-------------|-------------|--------------|
| Zn-N-C-1-700 | 59.34 | 20.6 | 12.03 | 8.02 |

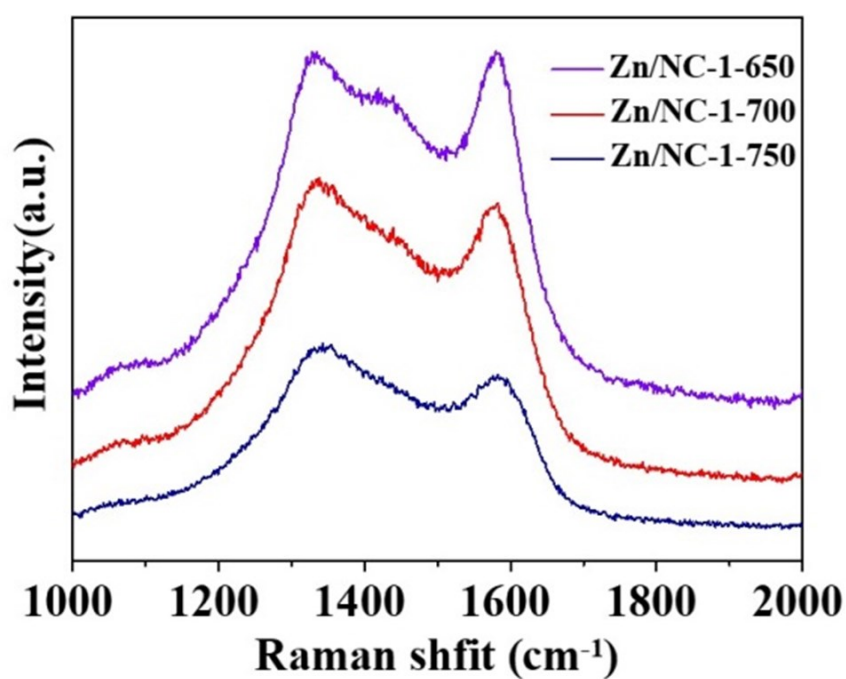


Fig. S5. (a) Raman spectra of Zn-N-C-1-700, Zn-N-C-1-750 and Zn-N-C-1-650.

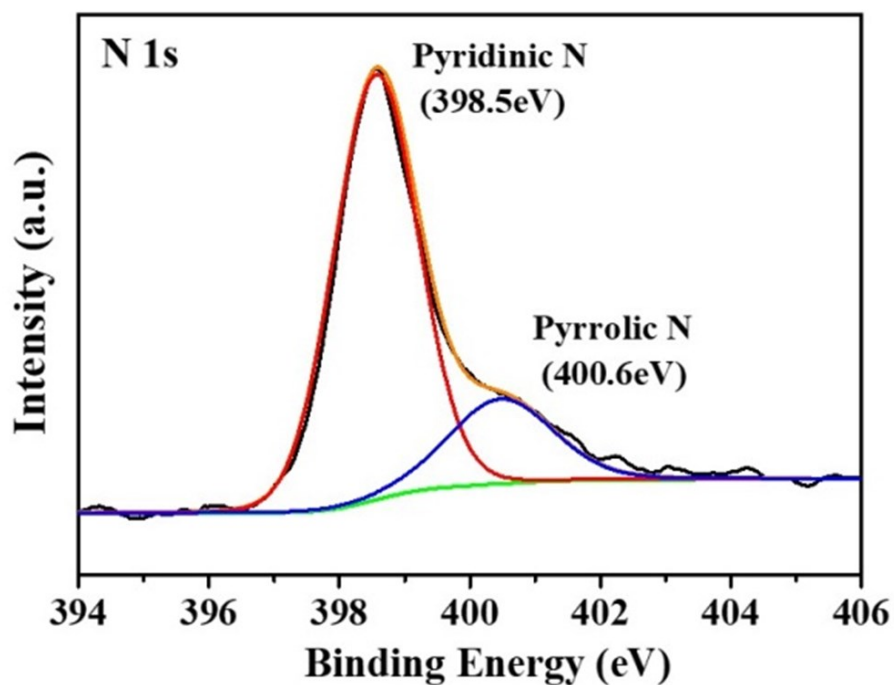


Fig. S6. (a) Raman spectra of Zn-N-C-1-700, Zn-N-C-1-750, and Zn-N-C-1-650; (b) XPS spectra of N 1s of Zn-N-C-1-700.

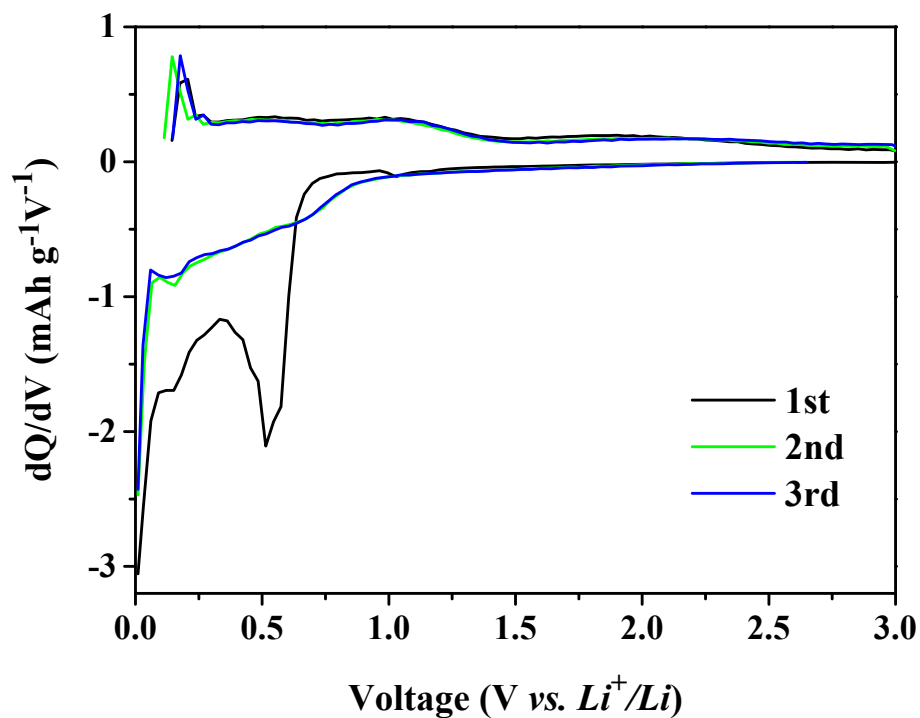


Fig. S7. Differential capacity plots of Zn-N-C-1-700. The peaks at 0.5 V and 0.1–0.35 V indicate the formation of SEI film and the alloying of Zn–N–C and Li.

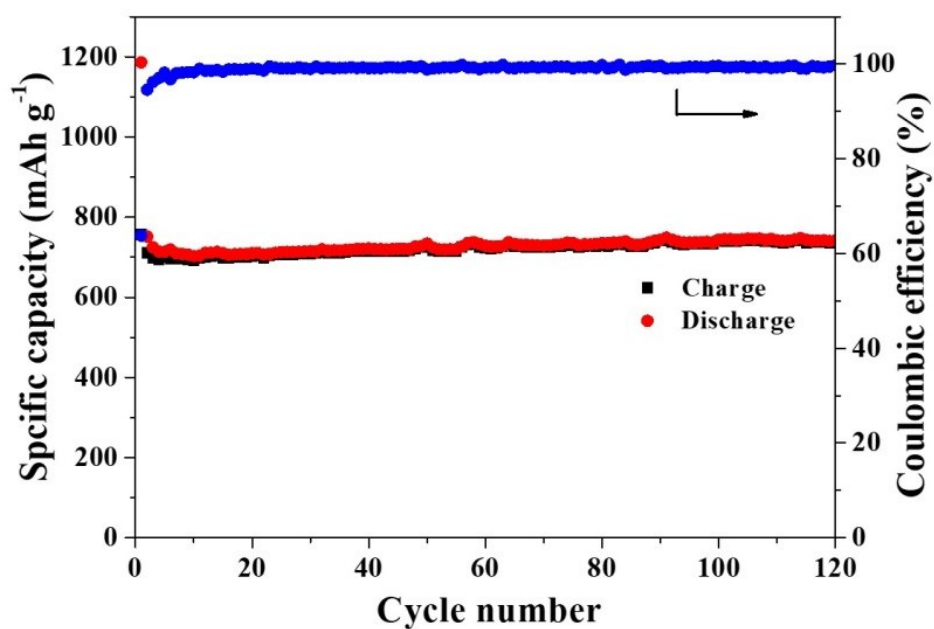


Fig. S8. Cycling performance of Zn-N-C-1-700 at the current density of 0.5 A g^{-1} and the corresponding Coulombic efficiency.

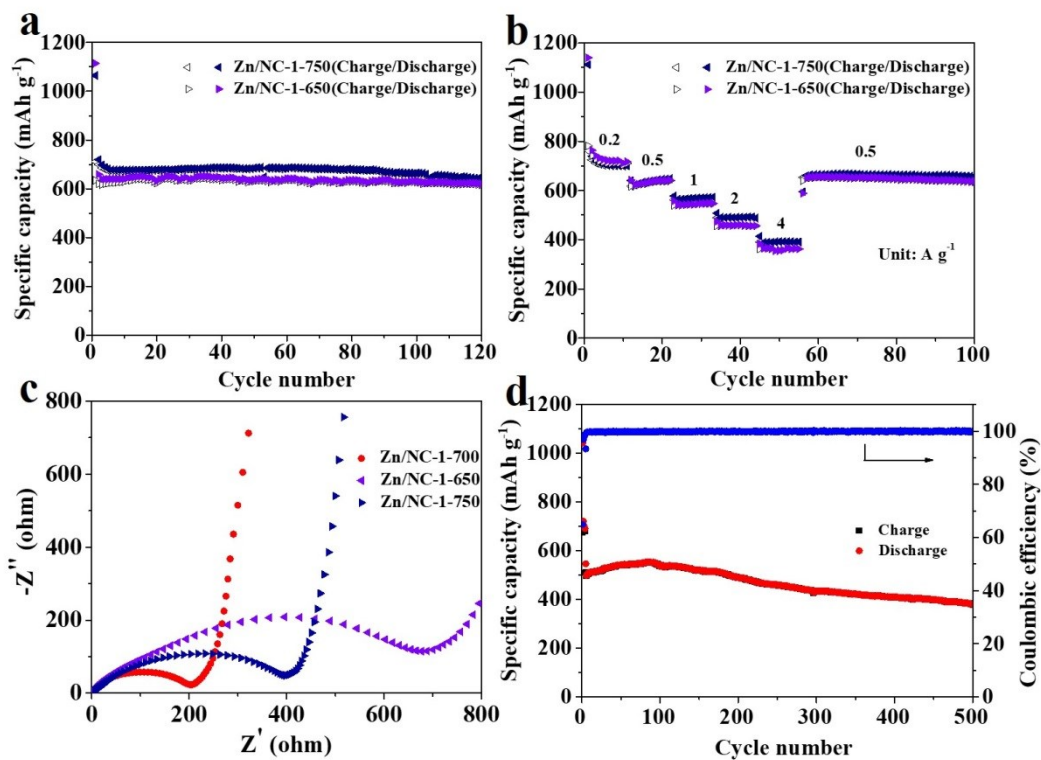


Fig. S9. (a) Cycling performance of Zn-N-C-1-700, Zn-N-C-1-650 and Zn-N-C-1-750 at the current density of 0.5 A g⁻¹; (b) Rate performance of Zn-N-C-1-700, Zn-N-C-1-650 and Zn-N-C-1-750; (c) EIS spectra of Zn-N-C-1-700, Zn-N-C-1-650 and Zn-N-C-1-750; (d) Cycling performance of Zn-N-C-1-700 at the current density of 2 A g⁻¹ and the corresponding Coulombic efficiency.

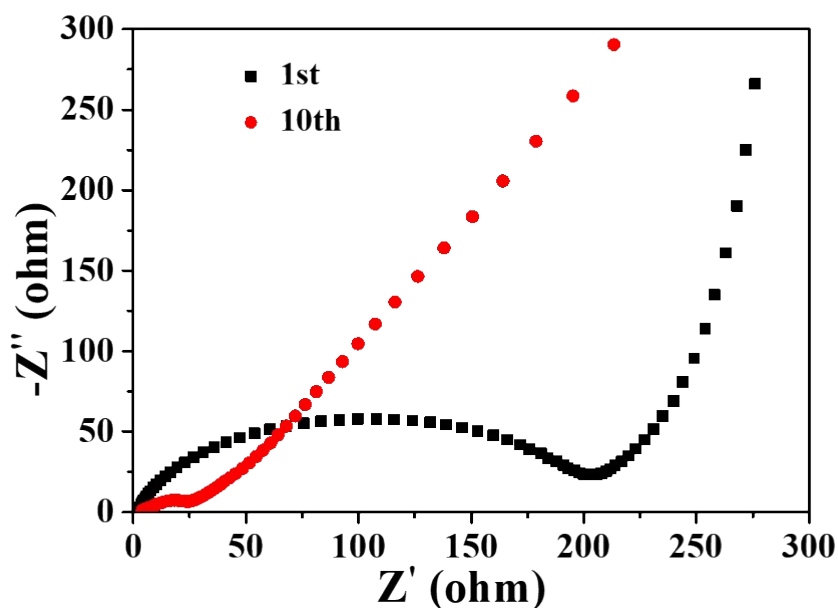


Fig. S10. EIS spectra of Zn-N-C-1-700 in the first cycle and tenth cycle.

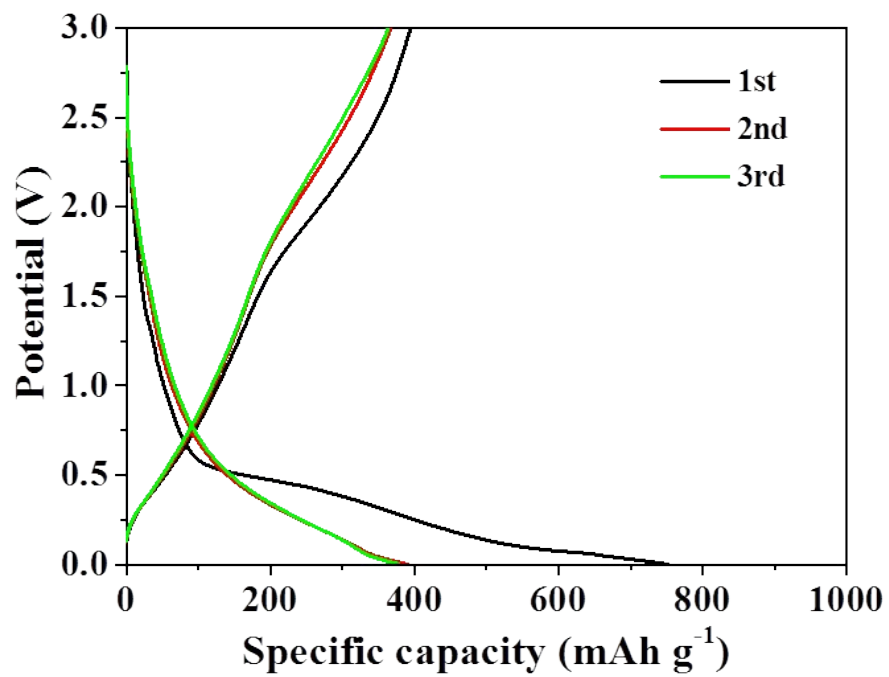


Fig. S11. Charge and discharge profiles of the N-C-1-700 at 0.5 A g⁻¹.